JOURNAL OF PETROLEUM AND GEOTHERMAL TECHNOLOGY
ISSN: 2723-0988, e-ISSN: 2723-1496

Vol. 7 No. 1 2026

Impact of Reservoir Horizontal Permeability Vertical Distribution on Recovery Efficiency Based on Deepwater Massive Sands

Azman Munthoha Maula [1*,2), Tsani Sabila [2), Putri Agustryani [1), Friska Hasugian [1), Dwi Miftha Kurnia [1), Randy Yusuf Kurniawan [1), Rozi Afdi [1)

[1)] Oil and Gas Engineering, Institut Teknologi Sumatera
[2)] Institute of GeoEnergy Engineering, Heriot-Watt University
* corresponding email: azman.maula@rmg.itera.ac.id

ABSTRACT

The influence of Deep-Water Massive Sands (DWMS) internal architecture on hydrocarbon recovery remains an area of ambiguity. This research endeavor aimed to elucidate the bed-scale ramifications of the vertical distribution of horizontal permeability, as determined from documented DWMS outcrop sedimentological analyses, on hydrocarbon recovery and sweep efficiency. This was achieved through the application of numerical waterflood simulations. Model construction leveraged outcrop textural parameters, including grain size, sorting, and orientation, in conjunction with analogous turbidite petrophysical subsurface data. The observed outcomes from four simulated heterogeneous cases revealed distinct trends in recovery efficiency, with variations up to 10%. These trends were attributable to the efficiency of water sweep and the interactive effects of vertical permeability heterogeneity, gravitational forces, and viscous forces. Specifically, the most stable, piston-like water sweep efficiency was associated with coarsening-upward permeability trends, followed by intermediate sweep efficiencies in anomalous and ungraded DWMS trends, and finally, the most unstable sweep efficiency in idealized trends.

Keywords: deep-water massive sands; permeability heterogeneity; recovery; sweep efficiency

I. INTRODUCTION

Deep-water massive sands (DWMS) are distinct, visually uniform, and structureless sedimentary beds resulting from deep-marine downslope processes (Stow and Johansson, 2000). These deposits are ubiquitous in the sedimentary record globally and frequently serve as major hydrocarbon reservoirs. Despite their substantial economic importance, the precise internal characteristics of DWMS and their subsequent influence on hydrocarbon recovery are not well understood.

This ambiguity in the internal character of DWMS poses a significant challenge for the petroleum industry, as it leads to considerable uncertainty regarding reservoir architecture and geological heterogeneity at various scales (Taira and Scholle, 1979; Hiscott and Middleton, 1980). Such heterogeneity directly impacts reservoir connectivity and fluid flow pathways, thereby influencing the ultimate hydrocarbon recovery factor, shaping field development strategies, and affecting project economics.

To mitigate these uncertainties, this project will develop bed-scale 2D reservoir models. These models will incorporate outcrop sediment texture data from a recent study on DWMS internal character trends (Patel et al., 2018; Maula et al., 2020), alongside published analogue petrophysical data. A series of waterflood numerical simulations will then be conducted on these models to systematically investigate the effect of bed-scale vertical variability in permeability and porosity on oil recovery efficiency, specifically within DWMS systems.

The overarching goal is to provide a more robust understanding of the characteristic reservoir recovery mechanisms in DWMS to support future development endeavors. In this paper, focus will be on impact of reservoir horizontal permeability vertical distribution on recovery efficiency.

1.1.1. Literature Review

1.1.2. Grain Size and Sorting

In sedimentary rocks, porosity and permeability are determined by both the initial sediment texture and the subsequent diagenetic history (Beard and Weyl, 1973). Porosity increases with increasing sorting (sorting has significant influence on porosity). Porosity is relatively flat with grain size changes. Permeability increases with increasing sorting. Permeability increases with increasing grain size.

1.1.3. Waterflooding in Deep-Water Massive Sands: Sweep Efficiency and Recovery

Water injection is a primary method for secondary oil recovery in the petroleum industry, favored for its cost-effectiveness, abundant supply, and superior stability compared to gas flooding. Waterflooding serves two key functions: maintaining reservoir pressure and displacing oil toward production wells. This project specifically focuses on the latter, investigating waterflood sweep efficiency in vertically heterogeneous Deep-Water Massive Sands (DWMS) systems and its implications for hydrocarbon recovery.

At the reservoir scale, waterflood sweep efficiency is governed by three main physical factors: mobility ratio, geological heterogeneity, and gravity (Dake, 2001). The mobility ratio (M), or end-point mobility ratio, is defined by **Equation 1**, where μ_w and μ_o represent the viscosities of water and oil, respectively, and k_{rw} and k_{ro} are their respective end-point relative permeabilities. While mobility ratio typically describes water sweep efficiency at the microscopic (pore) scale, it will remain constant in this numerical simulation study. This is because fluid viscosities are not varied, and relative permeability endpoints are kept consistent. The mobility ratio will be maintained near unity to ensure a stable waterfront.

$$M = \left(\frac{k_{rw}}{\mu_w}\right) / \left(\frac{k_{ro}}{\mu_o}\right) \quad (1)$$

1.1.4. Effect of variability in permeability vertical distribution on fluid flow

Permeability, particularly its degree of vertical variation, is by far the most significant factor influencing vertical sweep efficiency in a reservoir (Dake, 2001). Permeability can change by several orders of magnitude within a few feet. When a parameter so crucial to fluid flow exhibits such variability, its influence on vertical sweep efficiency tends to significantly outweigh that of other linked heterogeneous parameters, like porosity and water saturation.

The vertical distribution of permeability directly affects whether gravity slumping in reservoirs is retarded or accelerated. Figure 1 illustrates and summarizes these permeability-gravity relationships and the resulting waterflood sweep patterns, assuming a constant average permeability *k* for each scenario (Dake, 2001; Amy et al., 2013).

Case (a): Coarsening Upward Permeability (Increasing Upward)

This scenario leads to a stable, piston-like displacement across the entire macroscopic reservoir section. Initially, most injected water flows through the higher permeability layers at the top of the reservoir. As the viscous driving force from the injector diminishes logarithmically with radial distance into the formation, gravity begins to dominate. The continuous influx of water at the top then slumps towards the base, establishing an overall perfectly stable and sharp flood front.

Case (b): Fining Upward Permeability (Decreasing Upward)

Conversely, this situation results in an unstable displacement. The majority of injected water flows along the base of the reservoir section. Being denser, the water remains at the bottom, leading to early water breakthrough at the producing wells and significant bypassed oil in the upper sections of the reservoir.

Case (c): Intermediate Permeability Trend (Increasing to Decreasing Upward)

This case represents an intermediate scenario between the two above. It yields a moderately efficient waterflood sweep pattern, characterized by stable, piston-like displacement in the lower part of the reservoir but slower oil recovery in the upper section.

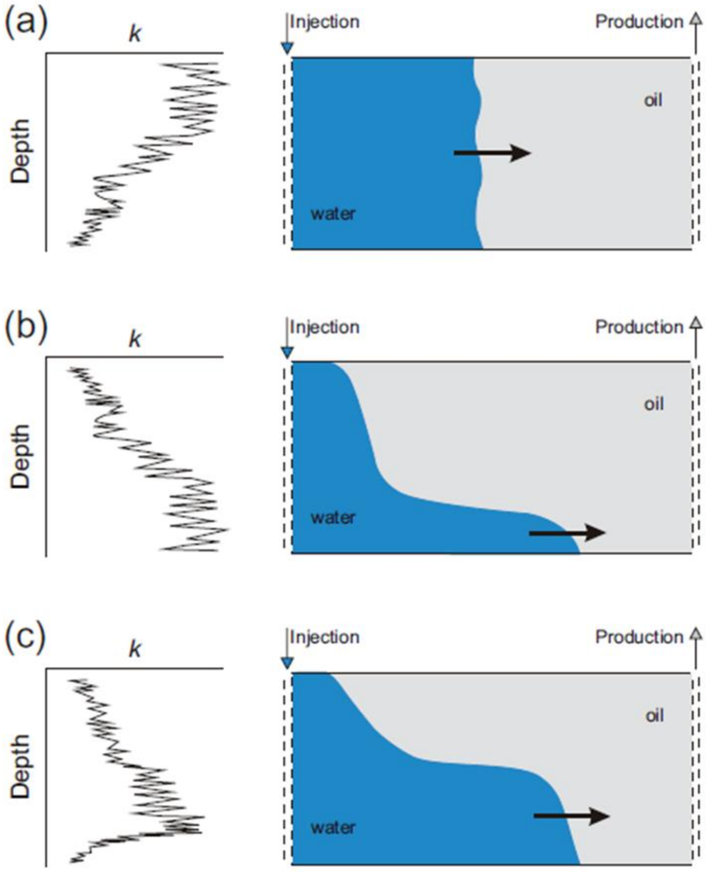

Figure 1. (a), (b), (c) : Reservoir-scale waterflood sweep patterns influenced by gravity and vertical permeability heterogeneity adapted from (Amy et al., 2013), redrawn from (Dake, 2001).

II. METHODS

Core reservoir management studies, which include sensitivity analysis, history matching, predictive forecasting, optimization, and uncertainty assessment, necessitate hundreds of numerical simulations (Maula et al., 2020). However, this section of the project focuses on defining and generating 28 heterogeneous simulation cases. These cases aim to address the project's primary objective: investigating how bed-scale vertical variations in porosity-permeability heterogeneity impact recovery efficiency in Deep-Water Massive Sands (DWMS).

The research methodology for this study is comprehensively outlined in Figure 2. The initial phase involved an extensive literature review, concentrating on Deep-Water Massive Sands (DWMS), the influence of sediment texture, waterflooding techniques, and the impact of heterogeneity on fluid flow. Following this, textural data was collected from outcrop samples to identify specific textural trends within DWMS.

The second stage focused on data conversion, translating the collected grain size and grain sorting data into porosity values using established relationships. Subsequently, permeability data was derived from these porosity values by applying poroperm correlations obtained from turbidite core samples.

The third stage comprised the development of a dynamic 2D numerical model, incorporating analogue subsurface data. The fourth stage involved the design and generation of multiple numerical model cases, each varying in geological heterogeneity parameters. These models were then simulated using IMEX, a black oil reservoir simulator from Computer Modelling Group (CMG).

Finally, the study concludes with the assessment of simulation results, specifically examining the impact of heterogeneity on waterflood sweep efficiency and recovery efficiency across different DWMS textural trends, with a comparative analysis against the idealized Bouma (1962) trend.

JOURNAL OF PETROLEUM AND GEOTHERMAL TECHNOLOGY
ISSN: 2723-0988, e-ISSN: 2723-1496
Vol. 7 No. 1 2026

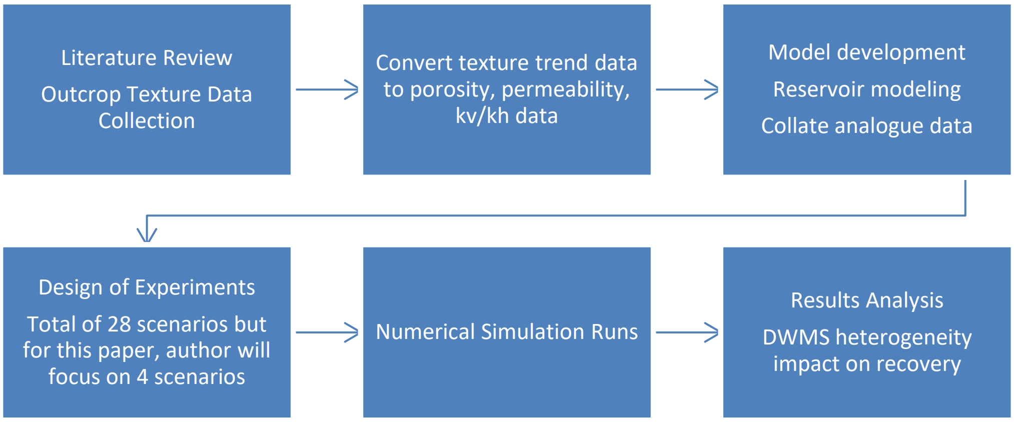

Figure 2. Research Methodology

There are four heterogeneity sensitivity series but for the focus will be directed at Series 1 of this study. Series 1 aims to investigate the impact of vertical permeability distribution variability as shown in Table 1. This involves constructing four distinct models that serve as base cases for all simulations, each representing a different vertical permeability trend. These include Trends 1-3 from Deep-Water Massive Sands (DWMS) and Trend 4, an idealized Bouma (1962) sequence.

Trend 4 was created by simply rearranging the data from Trends 1-3 into a fining-upward succession. Notably, permeability data revealed that Trend 3 exhibited a coarsening-upward trend due to improved sorting towards the top of the bed. For all models, it was assumed that vertical reservoir layer properties would be assigned the same value as the sample data points, based on an equidistant distribution between those points.

Table 1. Heterogeneity sensitivity series for simulation cases

Case ID	Layers	ϕ	k_h(mD)	k_v(mD)
Series 1: Sensitivity on horizontal permeability vertical distribution				
1-1	1-2	0.335	985.5683	396.1985
	3-8	0.3033	385.6135	352.0651
	9-13	0.3372	1048.387	813.5481
	14-17	0.3027	378.4724	365.6043
	18-20	0.337	1042.532	398.2471
1-2	1-2	0.3387	1093.246	1005.786
	3-6	0.3364	1025.141	902.1243
	7-12	0.33806	1073.9	558.4281
	13-17	0.336	1013.692	512.9283
	18-20	0.34	1133.503	136.0204
1-3	1-2	0.331385	889.6158	172.3186
	3-8	0.31283	516.4002	180.7401
	9-14	0.28992	251.877	27.70647
	15-17	0.292846	276.917	117.9666
	18-20	0.294928	296.069	136.1918
1-4	1-2	0.28992	251.877	27.70647
	3	0.292846	276.917	117.9666
	4	0.294928	296.069	136.1918
	5	0.3027	378.4724	365.6043
	6-7	0.3033	385.6135	352.0651
	8-9	0.31283	516.4002	180.7401
	10	0.3253	813.5171	564.0269
	11	0.331385	889.6158	172.3186
	12	0.335	985.5683	396.1985
	13	0.336	1013.692	512.9283
	14	0.3364	1025.141	902.1243
	15	0.337	1042.532	398.2471
	16	0.3372	1048.387	813.5481
	17-18	0.33806	1073.9	558.4281
	19	0.3387	1093.246	1005.786
	20	0.34	1133.503	136.0204

III. RESULTS AND DISCUSSION

Before analyzing the flow simulation results, it's crucial to understand the vertical distribution of horizontal permeability trends within the models. This is because, as documented in the literature, vertical permeability heterogeneity significantly impacts waterflood fluid flow behavior (Dake, 2001). Table 2, which presents the arithmetic average absolute horizontal permeability and the coefficient of variation (Cv) for each case in Series 1 (Patel et al., 2018), will be valuable for the subsequent analysis of these cases.

Table 2: Arithmetic average of horizontal permeability, Cv for Series 1 cases

Case	$\bar{k}h_{ar}$	Cv
1-1	708.412	0.472
1-2	1059.971	0.041
1-3	405.393	0.496
1-4	722.612	0.481

3.1. Analysis of Permeability Trends in Series 1

Table 2 (Series 1) provides a detailed overview of the four permeability trends investigated.

Trend 1 exhibits an irregular, anomalous vertical distribution, fluctuating from high to low, then high, low, and finally high permeability upwards. It has an average permeability of 708 mD and a coefficient of variation (Cv) of 0.47, indicating borderline homogeneity.

Trend 2 is characterized by a homogeneous, ungraded trend with a very low Cv of 0.04, reflecting its uniformity. This trend also shows the highest average absolute horizontal permeability at 1060 mD.

Trend 3 displays a distinct pattern: low permeability layers from the base to mid-depth, followed by a succession of higher permeability layers towards the top, essentially forming a coarsening-upward trend. This model also has the lowest average permeability at 405 mD and a nearly heterogeneous Cv of 0.496.

Finally, Trend 4, the idealized model, represents an even, graded succession of high to low permeability layers upwards, consistent with a fining-upward trend. Its average permeability of 722 mD is similar to Trend 1, with a Cv of 0.48.

3.2. Analysis of Oil Recovery Performance in Series 1

From Figure 3 (Series 1 plots, a and b), we can rank oil recoveries from highest to lowest at 0.6 pore volumes injected (PVI). This specific PVI was chosen as the analysis endpoint because Figure 3b clearly shows that after 0.6 PVI, the water cut for all models (and all subsequent scenario cases) consistently exceeds 90%, indicating a point of diminishing returns for oil production.

Based on this fixed analysis point, the results demonstrate the following recovery ranking: Trend 2 (Case 1-2) achieved the highest recovery, followed by Trend 1 (Case 1-1). Trend 3 (Case 1-3) showed slightly lower recovery, and Trend 4 (Case 1-4) had the lowest recovery among the series.

3.3. Explaining Recovery Trends in Series 1

The observed recovery trends can be supported by analyzing Table 2 (arithmetic average of horizontal permeability and coefficient of variation for Series 1) and the saturation profiles presented in Figure 4 (a) Trend 1, (b) Trend 2, (c) Trend 3, (d) Trend 4.

From the values in Table 2, it appears that viscous forces and permeability heterogeneity are the dominant factors influencing fluid flow in this waterflood displacement scenario, rather than gravity. This is evidenced by Trend 2's highest average permeability and corresponding highest recovery, despite its homogeneous ungraded nature.

However, a notable difference in recovery exists between Trend 1 and Trend 3, even with their significant disparity in average permeability. This can be attributed to the enhanced water sweep efficiency in Trend 3, which is facilitated by its coarsening-upward trend of increasing permeability layers vertically.

Similarly, while Trend 1 and Trend 4 have comparable average permeability values, their recoveries differ considerably. This discrepancy is due to the inefficient sweep mechanism in Trend 4, which is driven by its characteristic fining-upward trend of decreasing permeability layers vertically.

The saturation profiles presented in Figure 4 (a-d) further support how the varying vertical distribution of horizontal permeability affects recovery and sweep efficiency. While all cases initially exhibit a stable microscopic displacement shock front due to an end-point mobility ratio less than unity, our focus here is on the saturation distributions within this front, or the vertical sweep across the reservoir section. These distributions reveal the macroscopic effects of gravity and geological heterogeneity. Despite Trend 2 achieving the highest recovery due to its higher average permeability and strong viscous drive, Trend 3 clearly demonstrates the most efficient waterflood front.

3.4. Analysis of Waterflood Sweep Efficiency Across Permeability Trends

As illustrated in Figure 4 (a-d), Trend 3 exhibits a remarkable stable, nearly piston-like water front displacement, effectively sweeping oil across the reservoir. This trend demonstrates the longest and most stable vertical water sweep across the entire reservoir section. This efficiency is attributed to the presence of higher permeability layers at the top of its coarsening-upward succession. This configuration ensures a more replenished viscous flow at the top, which in turn mitigates the effects of gravity slumping to the base, resulting in a more optimally and equally distributed sweep.

Trend 2 shows the second-best sweep efficiency, characterized by a slightly higher water flood front compared to Trend 1 (Figure 4a). This improved sweep in Trend 2 is due to the presence of greater permeability layers towards its top. Both Trend 1 and Trend 2 generally result in an intermediate water sweep efficiency pattern, featuring a stable, piston-like displacement at the base but slower oil recovery in the upper section.

Conversely, the idealized Trend 4 model (Figure 4a) displays the least efficient sweep, marked by the lowest water flood front height and the most pronounced gravity slumping effect. This leads to earlier water breakthrough and consequently lower oil recovery. This poor performance is a direct result of its fining-upward succession, where the most permeable layers are located at the base.

This allows water to flow freely and remain at the bottom due to gravity, creating an unstable flood front displacement. These observations align with similar recovery trends noted in stratified reservoirs comparing idealized coarsening-upward and fining-upward models (Permadi et al., 2004).

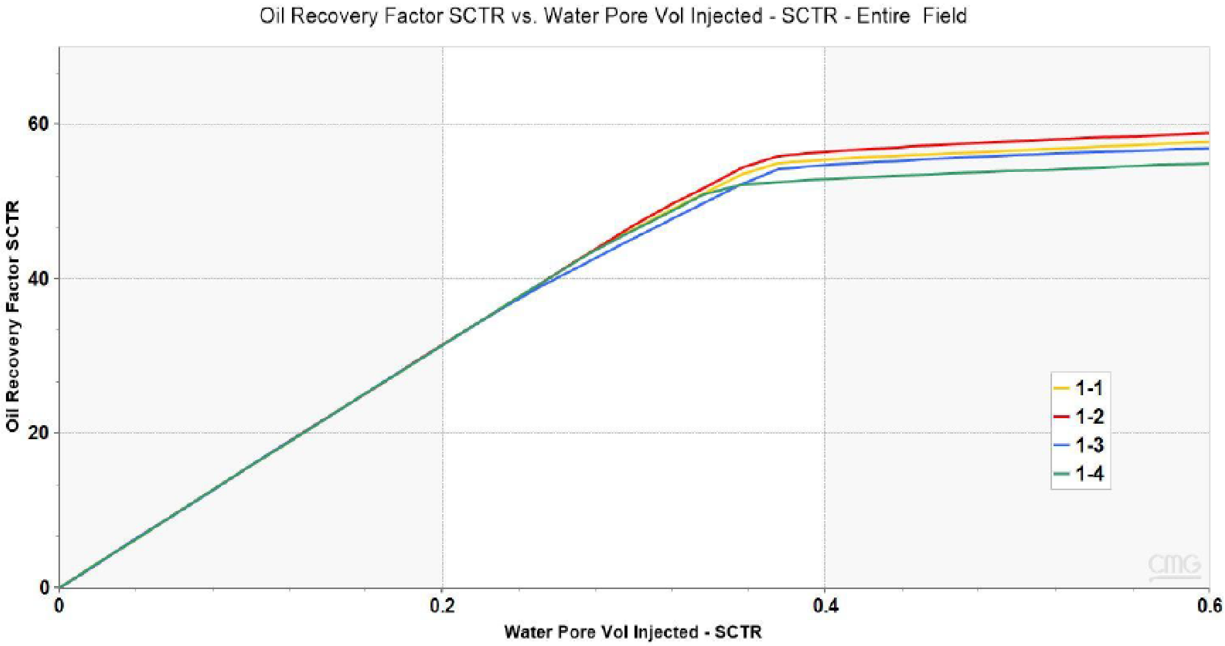

Figure 3(a). Oil recovery factor vs Pore volume injected. (Series 1 Plots)

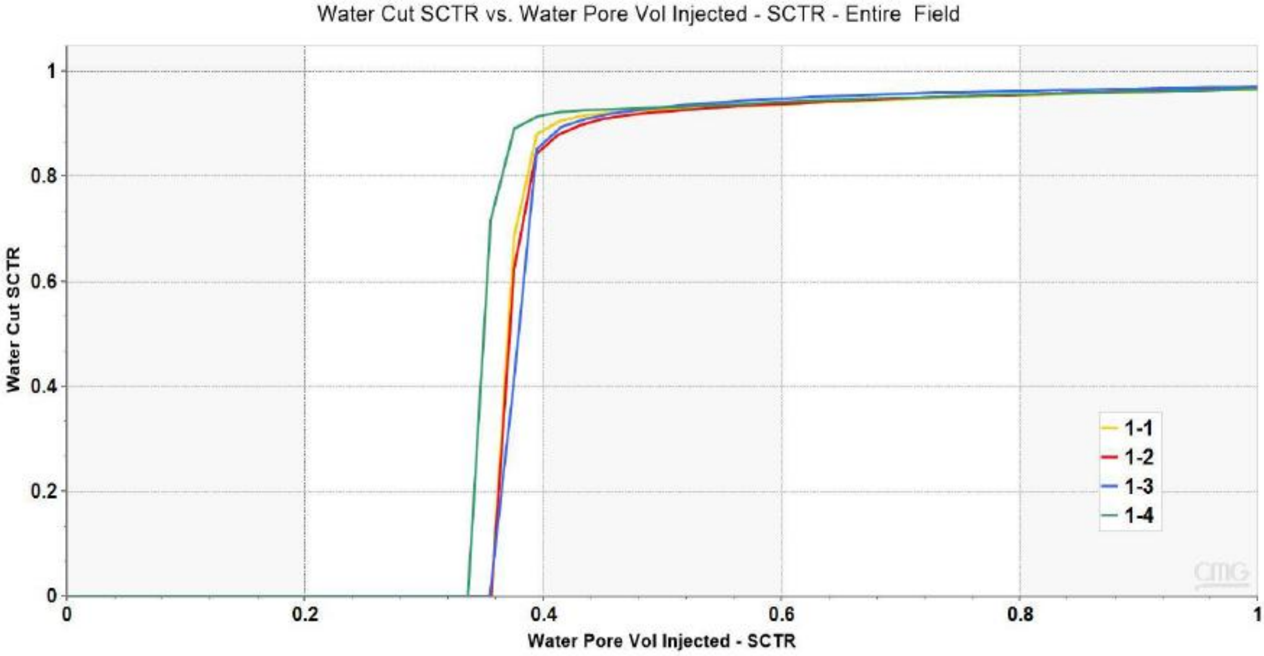

Figure 3(b). Water cut vs Pore volume injected.
(Series 1 Plots)

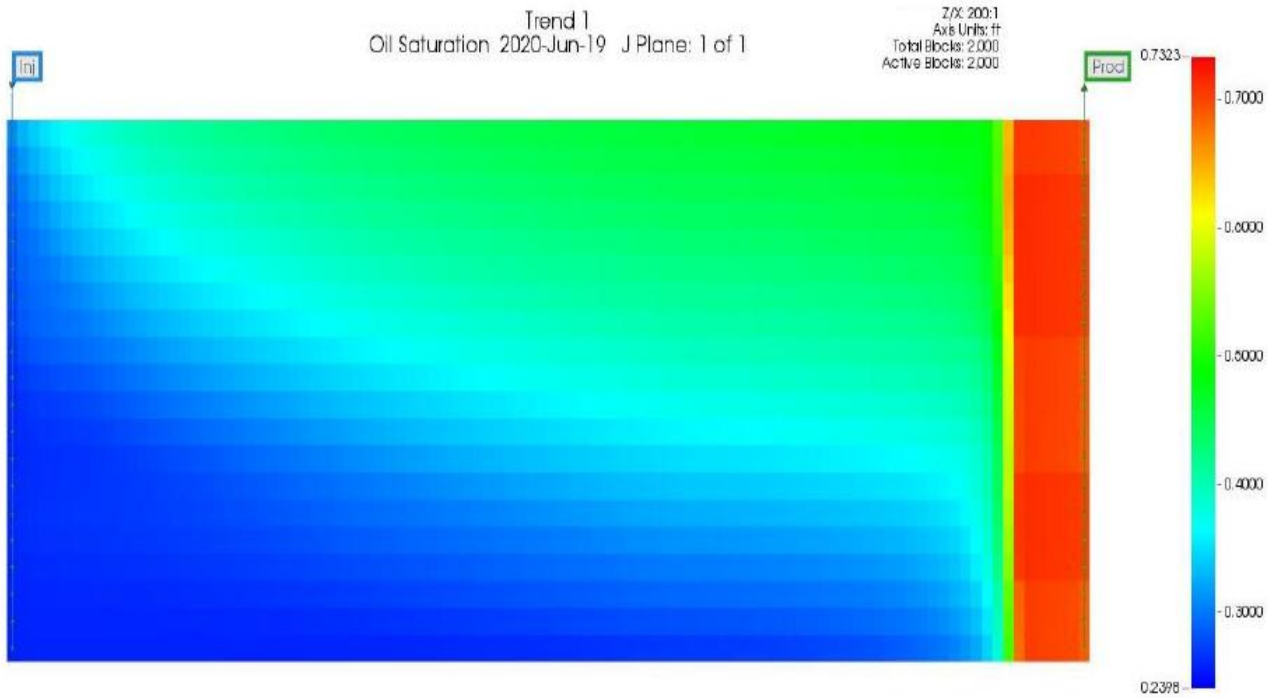

Figure 4(a). Trend 1, Saturation profiles of the 4 characteristic Trends in 2D reservoir cross-section view.

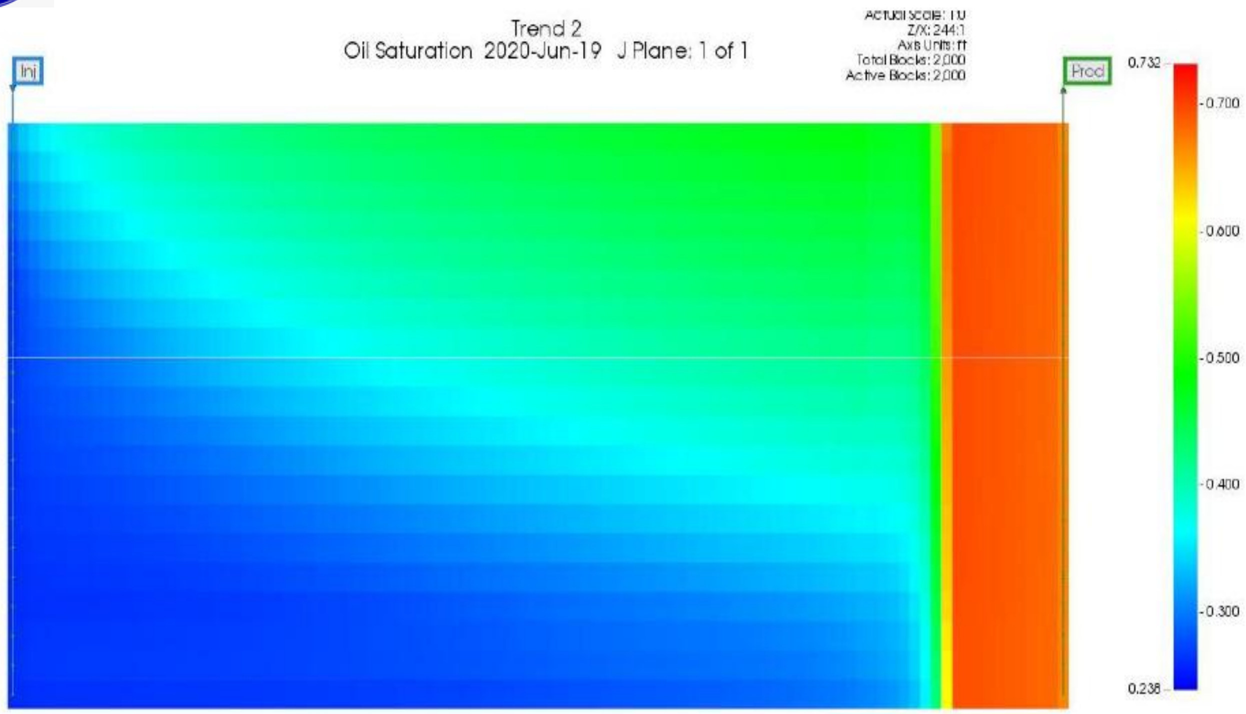

Figure 4(b). Trend 2, Saturation profiles of the 4 characteristic Trends in 2D reservoir cross-section view.

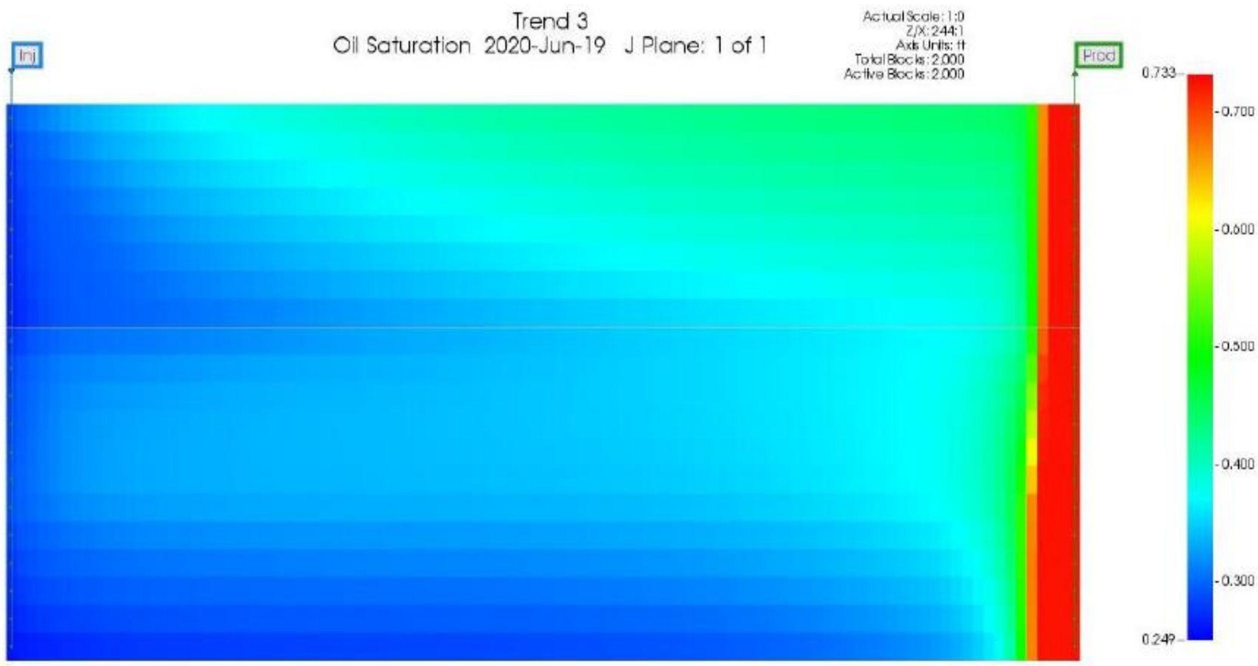

Figure 4(c). Trend 3, Saturation profiles of the 4 characteristic Trends in 2D reservoir cross-section view.

JOURNAL OF PETROLEUM AND GEOTHERMAL TECHNOLOGY
ISSN: 2723-0988, e-ISSN: 2723-1496
Vol. 7 No. 1 2026

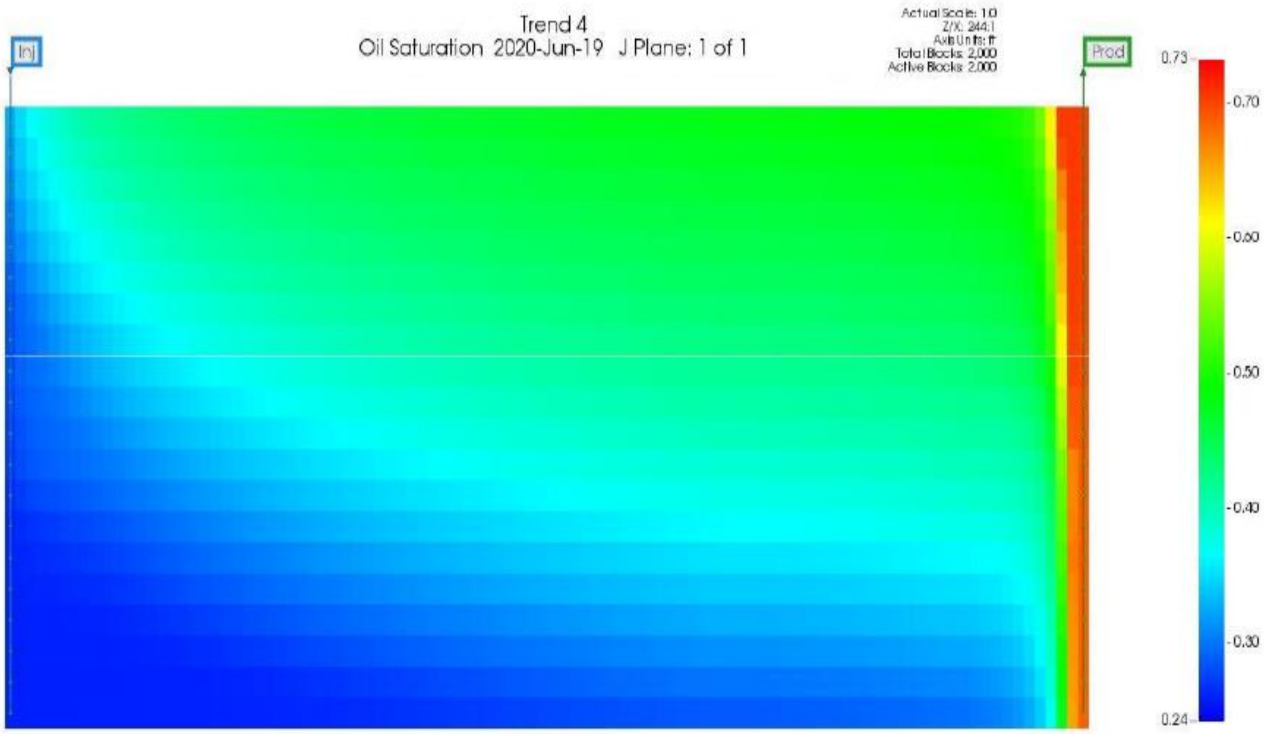

Figure 4(d). Trend 4, Saturation profiles of the 4 characteristic Trends in 2D reservoir cross-section view.

IV. CONCLUSION

The focus on this paper was the impact of reservoir horizontal permeability vertical distribution on recovery efficiency based on deepwater massive sands. Recovery efficiency of simulated cases resulted in a 10% difference. In summary, the vertical distribution of permeability significantly impacts oil recovery. The most stable, piston-like water sweep efficiency was observed in coarsening-upward trends. This was followed by intermediate sweep efficiencies in both anomalous and ungraded Deep-Water Massive Sands (DWMS) trends. Finally, the idealized trend consistently exhibited the most unstable sweep efficiency, leading to lower recovery. In line with the project's objectives, 2D waterflood reservoir simulation models were successfully developed. These models incorporated outcrop textural data, specifically grain size, grain sorting, and grain orientation, combined with analogue turbidite subsurface data.

This project operates under specific assumptions and limitations: (1) Assumption: It's assumed that diagenesis (post-depositional changes to the rock) did not significantly alter the primary porosity, meaning the original depositional controls on porosity are still observable. (2) Limitation: The study is restricted to analyzing sediment textural components—specifically grain size, grain sorting, and grain fabric (grain orientation)—for the Deep-Water Massive Sands (DWMS) textural trend analysis.

Recommended future works involve the lateral continuity of these models. The study revealed that the rate of production and injection, as well as the overall inter-well fluid front rate, significantly influenced the recovery response from these trends, indicating a strong rate dependency in the results.

REFERENCES

Amy, L., Peachey, S., Gardiner, A., Pickup, G., Mackay, E. & Stephen, K. (2013). Recovery efficiency from a turbidite sheet system: Numerical simulation of waterflooding using outcrop-based geological models. Petroleum Geoscience, 19, 123-138.

Beard, D. C. & Weyl, P. K. (1973). Influence of texture on porosity and permeability of unconsolidated sand. AAPG Bull., 349-369.

Bouma, A. H. (1962). Sedimentology of some flysch deposits. A graphic approach to facies interpretation, 168.

Dake, L. P. (2001). The Practice of Reservoir Engineering (Revised Edition), Elsevier Science.

Hiscott, R. N. & Middleton, G. V. (1980). Fabric of coarse deep-water sandstones, Tourelle Formation, Quebec, Canada. Journal of sedimentary research, 703-721.

Maula, A. M., Patel., U. S., Hamdi, Z. (2020). Impact Of Bed-Scale Heterogeneity On Recovery Efficiency In Deep-Water Massive Sands. Heriot-Watt University; Energy, Geoscience, Infrastructure and Society.

Maula, A., Rofieq, S., Sabila, T., & Lestariono, Y. (2020, October). Artificial neural network surrogate reservoir proxy modeling for generating pressure and gas saturation at the grid–block level in shale gas reservoirs. In Offshore Technology Conference Asia (p. D012S001R094). OTC.

Patel, U. S., Gardiner, A. R. & Stow, D. A. V. (2018). Deep Water Massive Sands : grain to depositional element scale analysis of their internal character. Heriot-Watt University; Energy, Geoscience, Infrastructure and Society.

Permadi, A., Yuwono, I. & Simanjuntak, J. (2004). Effects of Vertical Heterogeneity on Waterflood Performance in Stratified Reservoirs: A Case Study in Bangko Field, Indonesia. Proceedings of the SPE Asia Pacific Conference on Integrated Modelling for Asset Management.

Stow, D. & Johansson, M. (2000). Deep-water massive sands: Nature, origin and hydrocarbon implications. Marine and Petroleum Geology, 17, 145-174.

Taira, A. & Scholle, P. A. (1979). Deposition of resedimented sandstone beds in the Pico Formation, Ventura Basin, California, as interpreted from magnetic fabric measurements. Geological Society of America Bulletin, 952-962.